EAI Endorsed Transactions on Energy Web Research Article **EAI.EU**

Power–hydrogen system configuration integrating an improved Honey Badger Algorithm and mixed-integer programming

Mingyuan Lai[1,*], Dandan Li[1], Guoxian Luo[2], Jieren Tan[3]

[1]Guangxi Power Grid Co., Ltd., Nanning 530012, China
[2]Baise Power Supply Bureau, Baise 533000, China
[3]China Energy Engineering Group Guangdong Electric Power Design Institute Co., Ltd., Guangzhou 510663, China

Abstract

INTRODUCTION: Wind power variability challenges system regulation as renewables expand. Hydrogen storage provides long-term balancing.
OBJECTIVES: To optimize the operation and configuration of a wind-storage-hydrogen-gas turbine system.
METHODS: An Improved Honey Badger Algorithm (IHBA) with chaotic mapping and nonlinear parameters was combined with Mixed-Integer Programming (MIP) in a bi-level framework.
RESULTS: Using real data from Eastern Inner Mongolia, IHBA achieved a fitness of 0.424, outperforming PSO, GA and original HBA by 20.3%, 14.9% and 8.0%. The optimal system included 47.9 MW wind, 94.3 MWh battery, 23.8 MW electrolyzer, 38.9 t H_2 storage, 13.7 MW fuel cell and 7.1 MW H_2-blended turbine, at a minimal cost of 4.57×10^8 CNY. Annual H_2 output reached 68,900 Nm^3, storage level 0.2-0.8, LCOE 0.438 CNY/kWh and payback period 18.4 years. Additionally, comparisons across multiple energy sources, sensitivity and robustness analyses, and ablation experiments indicate that the system configuration is stable and the algorithm optimization performs reliably, providing a solid reference for design.
CONCLUSION: The IHBA-MIP framework is efficient and cost-effective for power-hydrogen system design, aiding large-scale renewable integration.

Keywords: capacity configuration, bi-level optimization, renewable energy integration, economic dispatch, system coordination

Received on 15 December 2025, accepted on 02 May 2026, published on 22 July 2026

doi: 10.4108/ew.14130

1. Introduction

The proportion of renewable energy in regional energy systems has continued to rise, and the increasing penetration of wind and photovoltaic (PV) power has disrupted the traditional energy balance. As a result, power systems must enhance their capability to accommodate high levels of renewable energy. Hydrogen production via electrolysis has become a key component of the energy transition, as renewable resources such as wind power can be converted into hydrogen due to their storable nature [1, 2]. Hydrogen storage tanks and fuel cells offer new opportunities for energy conversion, and integrated wind–storage–hydrogen–gas turbine systems help improve energy self-sufficiency, smooth power fluctuations, and enhance grid regulation, demonstrating strong feasibility. Capacity configuration and operational strategies exert significant impacts on system economics; the investment scale, operating characteristics, and coupling relationships among devices are highly complex, and different capacity choices can lead to entirely different operational modes [3, 4]. System planning often focuses on life-cycle cost. Looking ahead to future power–hydrogen coupling models, it is essential to conduct joint optimization research

*Corresponding author. Email: MingyuanLai@outlook.com

involving system-level design and operational mechanisms to support emerging power–hydrogen system architectures.

Extensive research has accumulated in the areas of wind–solar–storage system planning, hydrogen supply-chain design, and integrated energy system optimization [5–7]. Due to its determinism and high solution accuracy, Mixed-Integer Programming (MIP) is commonly applied to operational optimization in complex energy systems. Avilés et al. using an MIP-based planning method, optimized production sequencing and preventive maintenance for different wood types in pulp mill scheduling. Applied to a Chilean factory, the method effectively reduced setup time and improved decision-making efficiency [8]. Thomas and Sela proposed a tunable mixed-integer linear programming framework that employs piecewise linear approximations and integer solving to address nonlinear hydraulic behavior in water-supply networks. The framework achieved accuracy comparable to the specialized software EPANET while significantly improving solution speed and demonstrated strong application potential through pump station scheduling cases [9]. At the level of capacity planning, the existence of discrete decision variables, combinatorial explosion problem and non-convex characteristics usually prompt the research to adopt intelligent optimization algorithms, such as particle swarm optimization (PSO), genetic algorithm (GA) and honey badger algorithm (HBA), to improve the computational efficiency [10, 11]. Modu et al. used Salp group algorithm to optimize an off-grid multi-energy system composed of solar energy, wind energy, biomass energy, hydrogen energy and battery energy storage. Through the rule-based energy management strategy, the reliability of the system is guaranteed, which provides a sustainable energy solution for the power shortage areas in Nigeria [12]. Xia et al. putted forward an optimization method for industrial power-hydrogen energy system, built a bilateral transaction model between producer and consumer, comprehensively considered the change of equipment cost and industrial demand, promoted the local consumption of renewable energy, and provided support for emission reduction and decarbonization in industrial field [13]. However, the existing research still has limitations in the integration of capacity planning and operation optimization: intelligent algorithm has the ability of global search, but it is difficult to accurately describe the operation logic of equipment; However, mixed integer programming (MIP) can accurately express operational constraints, but it is difficult to directly deal with large-scale discrete capacity combination. This separation makes it difficult to realize the organic unity of capacity allocation and operation strategy, and thus it is difficult to ensure the overall optimization and economy, which still needs further study.

In order to meet the above challenges, this study constructs a capacity allocation method based on IHBA and an operation optimization method based on MIP, and further constructs a two-level optimization architecture that integrates them. IHBA undertakes capacity-level exploration, using Bernoulli chaotic mapping in the initialization phase to enhance population distribution uniformity, adopting a piecewise nonlinear decreasing parameter to adjust exploration intensity during the search process, and applying a lateral crossover mechanism to broaden the exploration space for capacity combinations. The MIP layer incorporates physical characteristics and operational logic of system components; through the MIP-based operational method, direct feedback is established between capacity decisions and operational costs, guiding the capacity search toward more economically favorable directions. Combining heuristic search and deterministic optimization, the two methods operate under a unified objective and form a continuous closed loop. The proposed bi-level structure offers an effective solution for planning wind–storage–hydrogen–gas turbine collaborative systems and provides an analytical framework for integrated optimization of capacity planning and operational control in power–hydrogen systems.

2. Method

2.1. Architecture of the wind–storage–hydrogen–gas turbine collaborative system

The wind–storage–hydrogen–gas turbine system is constructed from multiple energy devices, each serving distinct functions in the conversion and utilization of multi-energy flows. Wind turbines exhibit high power output during strong-wind periods, converting wind energy into electricity that can directly meet system loads. Variations in wind speed during these periods exert significant influence on the system's operating state [14, 15]. Gas turbines and hydrogen-doped gas turbines are used as compensation power sources, which operate under the condition of low wind speed or during the increase of power grid demand to reduce energy shortage or excess, thus partially smoothing the power fluctuation of the system. Hydrogen-doped gas turbines introduce a certain proportion of hydrogen into the natural gas combustion process, thus reducing carbon emissions and enhancing the clean energy properties of the system. As an energy buffer device, the battery energy storage system absorbs excess wind power during strong wind, and releases the stored energy when the load increases or the wind power decreases, so as to keep the stability of the load curve.

The hydrogen energy module includes hydrogen production, hydrogen storage and hydrogen power conversion equipment. Supercapacitor-alkaline electrolyzer (SC-ALK) is based on advanced alkaline electrolysis technology, which is very suitable for dealing with the long-term variability of wind power generation, and is used to convert excess wind energy into hydrogen. The electrolyzer absorbs excess wind and generates hydrogen, which is stored in a hydrogen tank. When the wind power is insufficient or the power grid demand increases, the system output can be adjusted upwards to adapt to the load change. The stored hydrogen is reconverted into electric energy by the fuel cell when needed. Fuel cell provides stable power output, which is suitable for the situation of rapid load change. SC-ALK cooperation subsystem reflects the characteristics of cross-media energy flow in multi-energy conversion chain, in which wind energy, electric energy and hydrogen energy change in different time ranges and maintain strong coupling.

The whole system structure consists of power generation subsystem and hydrogen storage subsystem. The power generation subsystem includes wind turbine, gas turbine, hydrogen-doped gas turbine and battery storage system. The hydrogen storage subsystem includes SC-ALK electrolyzer, hydrogen storage tank and fuel cell. System operation focuses on wind-power integration, power surplus and deficit management, hydrogen storage, and economic performance. When wind resources are abundant, wind power is directly fed into the grid to support the load, while the battery energy storage system performs peak shaving and valley filling; surplus wind energy is routed to the electrolyzer for hydrogen production. The produced hydrogen is stored in tanks and, in this study, primarily used for sale, with hydrogen sales revenue incorporated into the system's economic assessment. During power deficits, gas turbines and hydrogen-blended gas turbines generate supplemental electricity to support the system. Under such operational arrangements, the wind–storage–hydrogen–gas turbine system achieves multi-path balancing of energy flows. The system's structural topology is illustrated in Figure 1, showing the energy flows among wind power generation, battery storage, electrolysis, hydrogen storage, and gas turbine power generation.

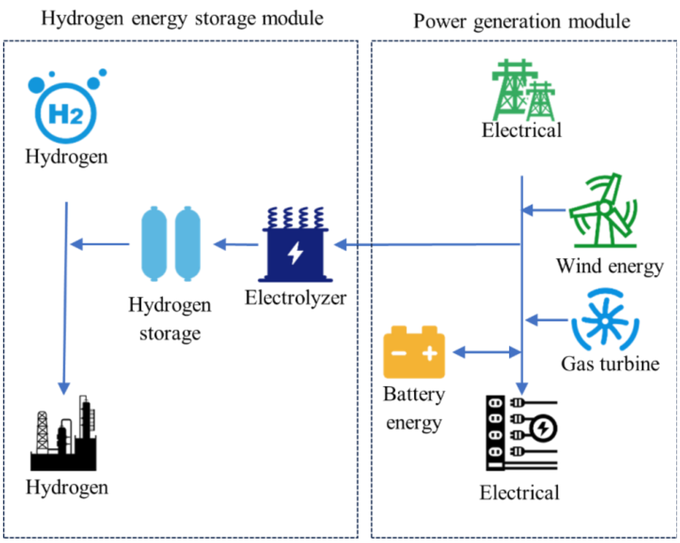

Figure 1. Structural topology of the wind–storage–hydrogen–gas turbine system

2.2. Mathematical model of the system

The mathematical model of the system was constructed based on the operational behavior of wind turbines, the battery energy storage system, the SC-ALK electrolyzer, hydrogen storage tanks, fuel cells, gas turbines, and hydrogen-blended gas turbines. Time was discretized into scheduling intervals $t \in \{1, \ldots, T\}$, and the variables included device power outputs, energy states, and on/off statuses. The total operating cost of the system includes power purchase and sales cost, natural gas consumption cost, start-stop cost, battery charging and discharging loss and hydrogen sales revenue. The goal of the model is to minimize the operation cost in the whole life cycle or scheduling cycle, under the premise of comprehensive consideration of economic benefits. The model is in the form of MIP, in which continuous variables are used to represent power and energy states, and binary variables are used to describe equipment start-stop and operation logic.

Objective function

The total system cost C included all expenses and revenues. Let λ_t^{buy} and λ_t^{sell} denote the electricity purchase and sale prices, λ^{H_2} the hydrogen sales price, and λ^{gas} the natural gas price. Hydrogen production from the electrolyzer is H_t^{ely}, hydrogen consumption by the fuel cell is H_t^{fc}, and natural gas consumed by the gas turbine/hydrogen-blended gas turbine is G_t^{GT}. The start-up event of the gas turbine is indicated by u_t^{start}, and the associated cost is C^{start}. The objective function is expressed as:

$$\min C = \sum_{t=1}^{T}(\lambda_t^{buy} P_t^{grid} - \lambda_t^{sell} P_t^{sell} + \lambda^{gas} G_t^{GT} - \lambda^{H_2} H_t^{ely}) + \sum_{t=1}^{T} C^{start} u_t^{start} \quad (1)$$

This function comprehensively considers the economic effects of power transaction, natural gas consumption, hydrogen revenue and start-stop behavior, and is used to characterize the overall operating cost of the system.

Constraints

The system constraints reflect the physical characteristics, energy balances, and logical relationships of each device. The wind turbine output is bounded by wind conditions and rated capacity: $0 \le P_t^{wind} \le P_t^{wind,max}$.

The energy state of the battery system E_t^{bat} depends on charging and discharging, with charging and discharging efficiencies η^{ch} and η^{dis}:

$$E_{t+1}^{bat} = E_t^{bat} + \eta^{ch} P_t^{ch} - \frac{P_t^{dis}}{\eta^{dis}} \quad (2)$$

The battery capacity constraint is $0 \le E_t^{bat} \le E_t^{bat,max}$.

The electrolyzer is constrained by rated power, and hydrogen production depends on its efficiency η^{ely}:

$$H_t^{ely} = \eta^{ely} P_t^{ely}, 0 \le P_t^{ely} \le P_t^{ely,max} \quad (3)$$

Hydrogen storage evolves according to production and fuel cell consumption, bounded by tank capacity:

$$H_{t+1}^{tank} = H_t^{tank} + H_t^{ely} - H_t^{fc}, 0 \le H_t^{tank} \le H_t^{tank,max} \quad (4)$$

The relationship between fuel cell power output and hydrogen consumption is given by:

$$H_t^{fc} = \frac{P_t^{fc}}{\eta^{fc}}, 0 \le P_t^{fc} \le P_t^{fc,max} \quad (5)$$

The output of the gas turbine or hydrogen-blended gas turbine is governed by the on/off status u_t: $0 \le P_t^{GT} \le u_t P_t^{GT,max}, u_t, u_t^{start} \in \{0,1\}, u_t^{start} \ge u_t - u_{t-1}$.

The system-wide energy balance is expressed as:

$$P_t^{wind} + P_t^{fc} + P_t^{GT} + P_t^{dis} + P_t^{grid} = P_t^{load} + P_t^{ely} + P_t^{ch} + P_t^{sell} \quad (6)$$

All continuous variables are restricted to non-negative values, and integer/binary variables must strictly take values of 0 or 1. The notation used in the above equations is summarized in Table 1.

Table 1. Symbols and their definitions

Symbol	Definition	Symbol	Definition
C	Total system operating cost, including electricity purchase/sales, gas consumption, start-up cost, and hydrogen revenue	C^{start}	Start-up cost of gas turbine (CNY/event)
λ_t^{buy}	Electricity purchase price at time (t) (CNY/kWh)	t	Index of scheduling interval
λ_t^{sell}	Electricity sale price at time (t) (CNY/kWh)	η^{ch}	Battery charging efficiency (0–1)
λ^{gas}	Natural gas price (CNY/m³)	η^{dis}	Battery discharging efficiency (0–1)
λ^{H_2}	Hydrogen sales price (CNY/kg)	η^{fc}	Fuel cell conversion efficiency (0–1)
P_t^{grid}	Power purchased from grid (kW)	η^{ely}	Electrolyzer efficiency (kg/kWh or kWh/kWh)
P_t^{sell}	Power sold to grid (kW)	H_t^{tank}	Hydrogen stored at time (t) (kg)
P_t^{ch}	Battery charging power (kW)	H_t^{fc}	Hydrogen consumed by fuel cell (kg)
P_t^{dis}	Battery discharging power (kW)	H_t^{ely}	Hydrogen produced by electrolyzer (kg)
P_t^{ely}	Electrolyzer power (kW)	E_t^{bat}	Battery energy state (kWh)
P_t^{fc}	Fuel cell output power (kW)	G_t^{GT}	Natural gas consumption (Nm³/h)
P_t^{wind}	Wind turbine power output (kW)	u_t	Binary on/off state of turbine
P_t^{GT}	Gas turbine/hydrogen-blended gas turbine power (kW)	u_t^{start}	Start-up indicator variable

2.3. Capacity optimization based on the IHBA

The system capacity optimization employed the IHBA as the core method, with the objective of generating the optimal capacity configuration for the wind–storage–hydrogen–gas turbine system. During initialization, the Bernoulli chaotic map was used in place of traditional random sampling to generate a more uniformly distributed initial population and enhance overall population diversity. Let the chaotic value of the n-th individual be z_n, updated as:

$$z_{n+1} = \begin{cases} \frac{z_n}{1-\varepsilon}, 0 \le z_n \le 1-\varepsilon \\ \frac{z_n-(1-\varepsilon)}{\varepsilon}, 1-\varepsilon < z_n \le 1 \end{cases} \quad (7)$$

where $\varepsilon \in [0,1]$ is a control parameter, and $n = 1,2,\dots,N$ denotes the index of each individual in the population. This method generates an initial capacity set that is uniformly distributed in the search space, thereby improving the convergence performance of the algorithm.

During algorithm iterations, an optimal-neighborhood strategy is employed to enhance local search capability [16, 17]. In IHBA, a piecewise nonlinear decreasing parameter is introduced to control the neighborhood size, which dynamically adjusts with the iteration step. Let δ_i denote the neighborhood parameter, $U(0,1)$ a random disturbance, and $\varphi_i(t)$ (t) the nonlinear decreasing coefficient. The neighborhood update is expressed as:

$$\delta_i(t) = \delta_i + \varphi_i(t) \times U(0,1) \quad (8)$$

The nonlinear decreasing coefficient $\varphi_i(t)$ is adjusted by quadratic curves with respect to the iteration number t. Examples include:

$$\varphi_1(t) = w_{max} - (w_{max} - w_{min}) \times (\frac{t}{T_{max}})^2 \quad (9)$$

$$\varphi_2(t) = w_{max} - (w_{max} - w_{min}) \times \frac{t}{T_{max}} \quad (10)$$

$$\varphi_3(t) = w_{max} - (w_{max} - w_{min}) \times [\frac{2t}{T_{max}} - (\frac{t}{T_{max}})^2] \quad (11)$$

where w_{max} and w_{min} are the maximum and minimum inertia weights, respectively, and T_{max} is the maximum number of algorithm iterations. The dynamic inertia weight ensures a smooth transition from global exploration to local exploitation, allowing the algorithm to avoid missing promising regions while refining local optima in later stages.

The HBA adopts an improved individual position update strategy in both the mining stage and the honey-seeking stage. During the digging phase, the position is updated by:

$$x_{new,i} = x_p \times \delta_i(t) + F \times \beta \times I \times x_p + F \times r_2 \times \theta \times d_i \times |\cos(2\pi r_3) \times [1 - \cos(2\pi r_4)]| \quad (12)$$

where $x_{new,i}$ is the updated position, x_p the current prey position, F a direction-correction factor, and r and d random disturbance terms. The coefficient β represents the disturbance-amplification factor during digging, I denotes the intensity of olfactory stimulation as the honey badger excavates prey, and θ controls the contribution of random disturbances during the search. In the honey-seeking phase, the position update is given by:

$$x_{new,i} = x_p \times \delta_i(t) + F \times r_6 \times \theta \times d_i \quad (13)$$

A lateral crossover strategy is incorporated during iteration to generate new solutions through interaction between two individuals, thereby expanding the search space and improving global search capability. The crossover equations are:

$$x_{new}(i) = a_1 \times x_i + (1 - a_1) \times x_j + a_2 \times (x_i - x_j) \quad (14)$$

$$x_{new}(j) = a_1 \times x_j + (1 - a_1) \times x_i + a_2 \times (x_j - x_i) \quad (15)$$

where x_i and x_j represent two parent individuals, a_1 is a random value in [0,1], and a_2 is a random value in [−1,1]. The resulting individuals $x_{new}(i)$ and $x_{new}(j)$ form part of the next population. Figure 2 illustrates the full workflow of the IHBA algorithm.

The capacity-allocation optimization process based on IHBA consists of the following steps: (1) set system parameters, upper and lower bounds for device capacities, and initialize the population, individual positions, and velocities; (2) compute the operating cost and fitness value of each individual; (3) identify preliminary local-best and global-best individuals. If the termination condition is satisfied, output the result and obtain the optimal system capacity; otherwise proceed as follows: (4) compute the intensity factor and density factor, generate a random number in [0,1], and determine whether the algorithm enters the digging phase or the honey-seeking phase; (5) update individual positions; (6) perform lateral crossover to obtain new solutions; (7) record the best solution and fitness value found so far; (8) iterate until the termination condition is satisfied and output the optimal capacity configuration.

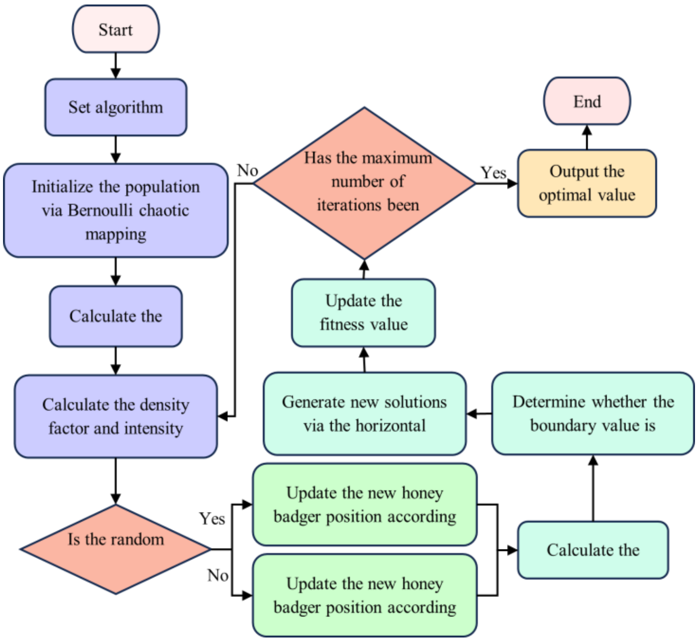

Figure 2. Flowchart of the IHBA algorithm

2.4. Dual-layer optimization framework of IHBA–MIP

The capacity planning and operational optimization of the wind–storage–hydrogen–gas turbine system exhibit strong nonlinearity, discreteness, and multi-objective characteristics, making it difficult for a single optimization method to simultaneously ensure global exploration capability and fine-grained local exploitation. To address these limitations, this study establishes a dual-layer optimization framework that integrates IHBA with MIP. In the upper layer, IHBA generates candidate capacity combinations through iterative updates. In the lower layer, a MIP model is constructed for each capacity combination to obtain the optimal operational strategy and compute the corresponding operating cost. The upper layer treats the operating cost fed back by the lower layer as the fitness function, guiding IHBA to search toward more cost-effective capacity regions. The iterative interaction between the two layers continues until the optimal capacity configuration and operational strategy are obtained, as illustrated in Figure 3.

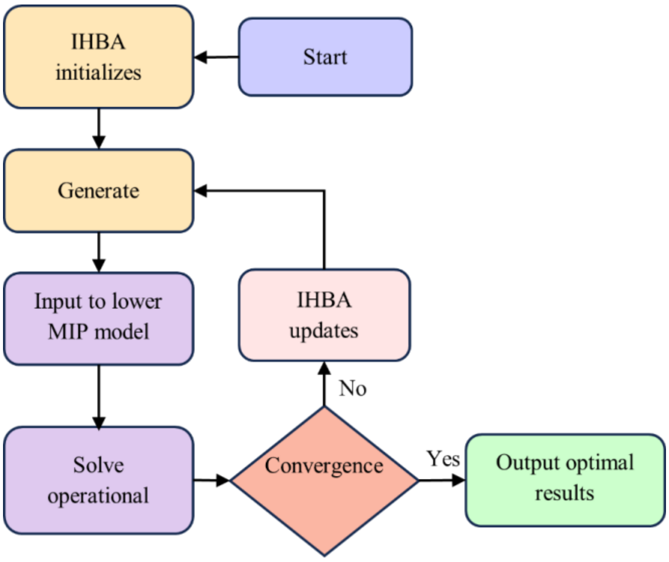

Figure 3. Flowchart of the IHBA-MIP Two-Layer Optimization Framework

In the upper-layer IHBA capacity optimization, the population is denoted as $X = \{x_1, x_2, \dots, x_N\}$, representing the set of individual capacity solutions. Each individual includes the capacities of wind turbines, gas turbines, hydrogen-mixed gas turbines, battery storage, and hydrogen storage tanks. Let $f(x_i)$ represent the lifecycle cost corresponding to individual x_i, which is calculated through the lower-layer MIP model. The capacity update formula can then be expressed as:

$$\min_{y_t} C(x_i, y_t)\,, \text{s.t.}\, \mathcal{G}(x_i, y_t) \le 0, \mathcal{H}(x_i, y_t) = 0 \qquad (16)$$

where $\mathcal{G}$ represents the set of inequality constraints, such as power bounds, energy-capacity limits, and binary decision constraints, and $\mathcal{H}$ represents the set of equality constraints, such as system energy-balance equations. The resulting operating cost $C(x_i, y_t^*)$ is returned to the upper-layer IHBA as the fitness value. The dual-layer iteration aims to minimize the total cost C_{total}, which can be formalized as:

$$C_{total} = \min_{x_i \in X} \{C(x_i, y_t^*(x_i))\} \qquad (17)$$

Through iterative interaction, the upper-layer IHBA optimizes the device capacities, while the lower-layer MIP derives the optimal operational strategy. This dual-layer architecture enables simultaneous identification of the optimal capacity combination and its corresponding cost-effective operational schedule. The pseudocode of the IHBA–MIP algorithm is presented in Figure 4.

```
Start
Input: System parameters, wind/ load data, IHBA parameters (population size N, max iterations T_max), device capacity bounds
Parameters: PDN = segmented nonlinear decreasing parameter, F = direction factor, c1, c2 = crossover random numbers
Output: Optimal device capacity x*, optimal operation strategy y*, minimum lifecycle cost C_total
Initialize IHBA population X = {x_1, x_2, ..., x_N} using Bernoulli chaotic mapping
Calculate initial fitness f(x_i) for each x_i via MIP model to get initial operation cost
Set initial global best x_p and local bests for each individual
For t = 1 to T_max do
    For each individual x_i in X do
        Compute strength factor and density factor
        Generate random number r in [0,1]
        If r < 0.5 then
            Update x_i using IHBA exploration (digging phase): x_i^new = x_i + PDN * F * r * (x_p - x_i)
        Else
```

Figure 4. IHBA-MIP algorithm pseudocode

2.5. Case study and parameter settings

A case study was conducted using the actual wind-power output data from a region in Eastern Inner Mongolia to optimize the configuration and operational control strategy of the wind–storage–hydrogen–gas turbine system shown in Figure 1. The objective is to maximize wind-power utilization, ensure that the energy storage system absorbs surplus power, rationally coordinate hydrogen production and use, and minimize overall economic cost, while guaranteeing the ability to meet load demand under large wind-power fluctuations. Wind power is prioritized to meet the load. The battery energy storage system absorbs short-term load fluctuations. When wind power exceeds the load, the surplus is directed to the electrolyzer for hydrogen production, which is then stored in the hydrogen tank. The fuel cell provides auxiliary power during periods of insufficient wind or during load peaks. The gas turbine supplies power for peak demand, ensures economic and stable system operation, and enhances flexibility under extreme load conditions. The hydrogen-blended gas turbine also reduces carbon emissions and increases the share of green energy. Hydrogen can also be sold externally, generating economic revenue. System parameters for the case study are listed in Table 2.

Table 2. Device and related parameter settings

Parameter	Value
Battery unit cost	630 yuan/kWh
Hydrogen-storage unit cost	65 yuan/kg
Maximum wind-power capacity	50 MW
Annual load	879,820 MWh
Electrolyzer efficiency	0.71
Electrolyzer lifetime	15 years

Parameter	Value
Electrolyzer unit cost	2210 yuan/kW
Electrolyzer replacement cost factor	0.15
Electrolyzer operating load	50%–100%
Wind-power price	0.2985 yuan/kWh
Gas-power price	0.512 yuan/kWh
Water price	3.32 yuan/ton
Natural gas price	1.22 yuan/m³
Life cycle	20 years
Discount rate	8%

The simulation platform was established in MATLAB R2023a, with the commercial solver Gurobi 9.5 integrated to solve the lower-layer MIP model. The upper-layer IHBA algorithm was developed using custom MATLAB code. The population size, maximum iteration number, and chaotic-mapping parameters were adjusted based on system scale, and the final settings are listed in Table 3. Both wind-power output and load data were obtained from historical operation data in Eastern Inner Mongolia with a temporal resolution of 1 hour to ensure realistic operational simulation.

Table 3. IHBA parameter settings

Parameter	Value
Population size	30
Maximum iterations	200
Bernoulli chaotic-mapping parameter	0.5
Piecewise nonlinear decreasing parameter	0–1
Direction-correction factor	1
Lateral crossover random numbers	0–1, −1–1
Convergence threshold	(10^{-4})

3. Results and discussion

3.1. Performance evaluation of the IHBA–MIP framework

To assess the effectiveness of IHBA in solving the capacity-allocation problem, its performance was compared with three representative intelligent optimization algorithms: PSO, GA, and HBA. All algorithms were executed with identical parameter settings, the same fitness function, and the same random seed. The evolution of the fitness value with respect to iteration number was recorded. A smaller fitness value indicates a lower system operating cost. The convergence trajectories of the algorithms are shown in Figure 5.

As shown in Figure 5, IHBA outperformed the other methods in both solution efficiency and convergence quality. In terms of convergence speed, the fitness value of IHBA had already decreased to 0.476 at the 50th iteration, which was significantly lower than HBA (0.586), GA (0.646), and PSO (0.663). In the 100th iteration, IHBA has reached 0.424, and it remains stable in the subsequent iterations, showing a faster convergence speed and higher convergence accuracy. In contrast, HBA converges to 0.467 after the 300th iteration, while GA and PSO stagnate at 0.498 and 0.536 respectively, which shows the characteristics of slow convergence and easy to fall into local optimum. In terms of the final fitness value, the 0.424 obtained by IHBA is 8.0%, 14.9% and 20.3% lower than that of HBA, GA and PSO, respectively, indicating that its overall optimization performance has been significantly improved. The above results show that IHBA has obvious advantages in global search ability, local development ability and convergence stability, and is suitable for capacity planning of complex energy systems.

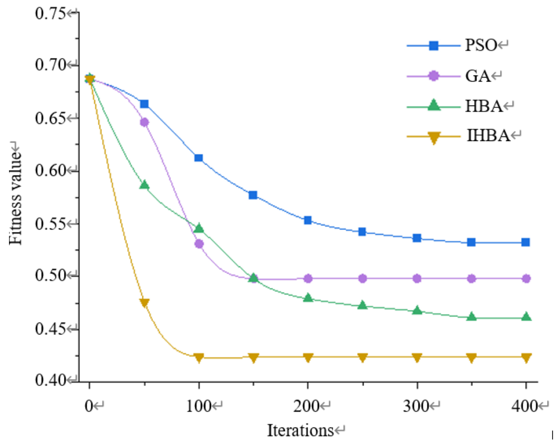

Figure 5. Fitness optimization process of each algorithm

Figure 6 shows the optimal capacity allocation results obtained by four optimization algorithms, including the installed capacity of wind power, the scale of battery energy storage, the capacity of electrolytic cell and fuel cell, and the capacity allocation of hydrogen storage tank and hydrogen-doped gas turbine.

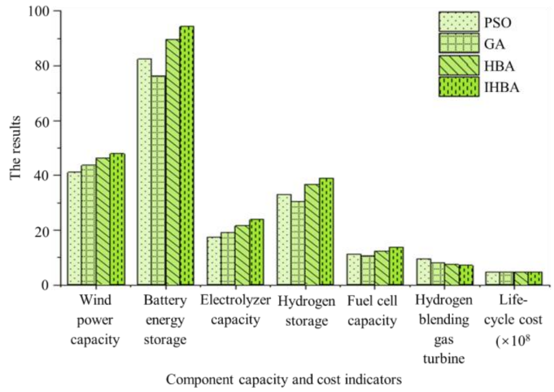

Figure 6. Comparison of optimal capacity configurations obtained by different algorithms

The results in Figure 6 show that different algorithms form a differentiated capacity combination scheme in the feasible domain. The solutions obtained by PSO and GA are relatively conservative. The installed capacity of wind power is 41.3 MW and 43.8 MW respectively, and the energy storage capacity of battery is 82.6 MWh and 76.4 MWh respectively, which are lower than the configuration level of HBA and IHBA. The search depth of HBA has been improved, and the installed capacity of wind power has been increased to 46.2 MW, while the capacity of electrolytic cell and hydrogen storage tank has reached 21.6 MW and 36.8 t respectively. IHBA showed stronger capacity coordination, increasing the capacity of wind power, energy storage and electrolyzer to 47.9 MW, 94.3 MWh and 23.8 MW respectively, and the scale of hydrogen energy subsystem also reached the maximum, while the capacity of hydrogen-doped gas turbine decreased to 7.1 MW, indicating its stronger renewable energy substitution capacity. In terms of total cost, IHBA achieves the lowest cost of 4.57× 10 yuan, which is 5.2% and 2.6% lower than PSO and HBA, respectively, which verifies the superiority of this method in capacity coupling coordination and economic performance optimization.

3.2. System operation analysis

To intuitively illustrate the hydrogen storage dynamics of the wind–storage–hydrogen–gas turbine collaborative system throughout the year, Figure 7 presents the monthly hydrogen production, hydrogen consumption, and the end-of-month State of Hydrogen (SOH).

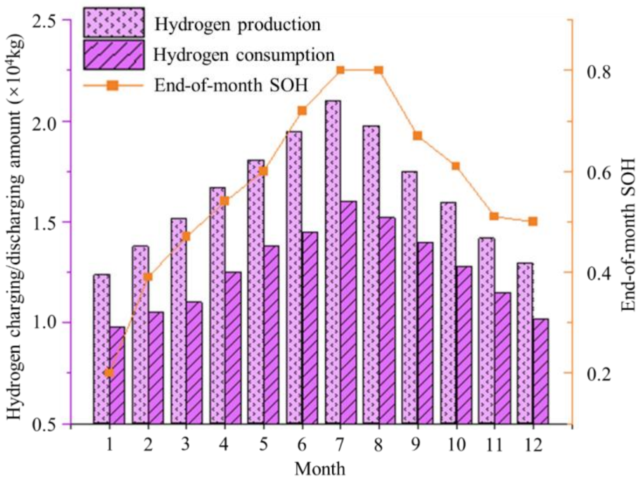

Figure 7. Annual variation of system hydrogen state

Figure 7 indicated that hydrogen production exhibited pronounced seasonal fluctuations. Due to abundant wind resources in summer, hydrogen production peaked in July at 2.10×10^4 kg, whereas the lowest value occurred in February at 1.30×10^4 kg. Hydrogen consumption closely followed load demand, reaching 1.60×10^4 kg in the high-load month of July and only 0.98×10^4 kg in the low-load month of January. The end-of-month SOH reflected the charging and discharging patterns of the hydrogen storage tank. The SOH peaked at 0.8 in summer and dropped to 0.2 in winter. Compared with the more significant peaks and troughs in hydrogen production, SOH exhibited smaller fluctuations, indicating that the fuel cell and hydrogen sales played key roles in regulating hydrogen storage levels. Throughout the year, SOH is always maintained at 0.2–0.8, which ensures sufficient reserve capacity during the surplus period of wind power and avoids the long-term full-load operation of hydrogen storage tanks. The results show that the system effectively balances wind power fluctuation and load change through hydrogen energy storage, and realizes the coordinated optimization of energy regulation and economic benefits.

The annual wind power output and wind abandonment are shown in Figure 8.

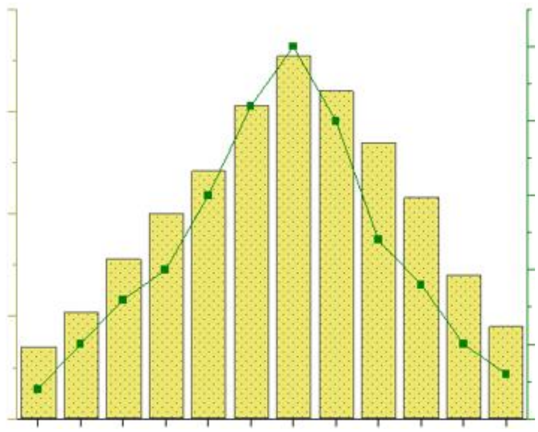

Figure 8. Annual wind power output and curtailment

As shown in Figure 8, the wind power output shows obvious seasonal variation characteristics, reaching a peak value of 42.7 MW in July and a minimum value of 28.5 MW in January. Battery energy storage and hydrogen energy storage modules smooth the fluctuation of wind power and reduce the level of wind abandonment to a certain extent, but there is still wind abandonment in the case of excessive wind power or low grid load. Among them, the maximum abandoned wind occurred in July, reaching 3.5×10^4 kWh, and the minimum abandoned wind was 1.2×10^4 kWh, which occurred in January. Generally speaking, the energy storage and hydrogen energy subsystem effectively alleviates the fluctuation of wind power, keeps the annual wind abandonment rate at a low level, and shows strong wind power absorption capacity and system adjustment capacity.

In order to further illustrate the dynamic characteristics of wind-storage-hydrogen-gas turbine system in typical operation period, Figure 9 shows the time-varying power output of electrolyzer, gas turbine and fuel cell, and the change of hydrogen storage level of hydrogen storage device.

As shown in Figure 9, the power of electrolyzer fluctuates with the change of wind power output, and when the wind power is abundant, the hydrogen production power increases rapidly, reaching the maximum of 44.8 MW. The output of fuel cell is adjusted according to the load demand, and the peak value is 23.6 MW, which shows good load following ability. The output of gas turbine is relatively stable, but it provides supplementary power at low wind speed or peak load, with a maximum output of 27.6 MW. The hydrogen storage level varies from 0.05 to 0.95, which indicates that the energy storage unit can effectively absorb surplus power and release it at peak load, thus maintaining the energy balance of the system. The results show that the electrolyzer, fuel cell and gas turbine work together, and the hydrogen storage unit plays a key role in the process of peak shaving and valley filling, thus improving the utilization rate of wind power and the stability of system operation.

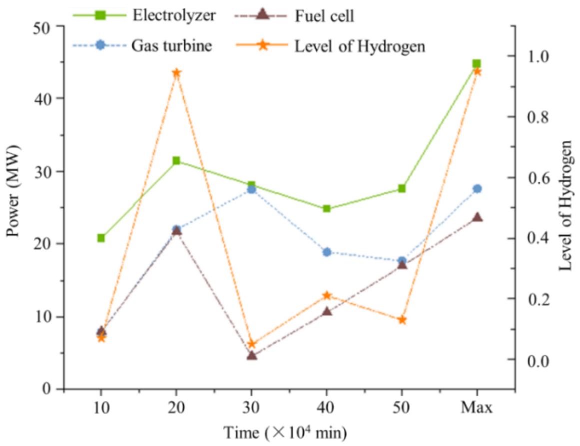

Figure 9. Operation of the hydrogen storage unit, fuel cell, electrolyzer, and gas turbine

3.3. Economic analysis

Scenario 1 corresponds to the wind-storage-hydrogen-gas turbine system under the action of operation control strategy, while scenario 2 represents the system without operation control strategy. The comparison results of LCOE, hydrogen production and dynamic payback period in two scenarios are shown in Figure 10.

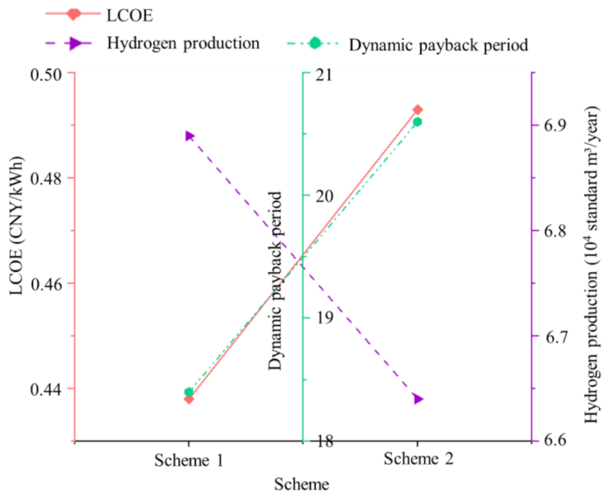

Figure 10. Economic Analysis Results

As shown in Figure 10, in Scenario 1, the LCOE is 0.438 CNY/kWh, which is lower than 0.493 CNY/kWh in Scenario 2, with a decrease of 11.2%. This shows that the operation control strategy can effectively optimize the scheduling process of power and energy storage, thus reducing the operating cost of the system. In terms of hydrogen production, the hydrogen production in scenario 1 reached 68,900 standard cubic meters, which was 3.8% higher than that in scenario 2, indicating that the optimized scheduling improved the utilization rate of electrolyzers and the hydrogen energy output capacity. In terms of dynamic investment payback period, Scenario 1 is 18.4 years, which is 2.2 years shorter than Scenario 2, reflecting a significant improvement in investment payback efficiency. Generally speaking, the introduction of operation control strategy not only improves the utilization efficiency of wind power and energy storage system, but also reduces the cost, improves the income and accelerates the investment recovery process, which verifies the key role of intelligent dispatching in economic optimization.

3.4. Multi-Energy Comparison Analysis

In order to verify the adaptability of IHBA-MIP framework in various renewable energy scenarios, a photovoltaic system was introduced to the original wind-storage-hydrogen-fuel cell (WSHF) system, and a comparative case was built. This study sets up three typical configuration modes: pure wind power system (Case 1), pure photovoltaic system (Case 2) and wind-solar complementary system (Case 3). Photovoltaic output data are generated based on typical annual irradiation data in the same area, and the time resolution (1 h) is the same as that of wind power data to ensure the fairness of comparison. In all scenarios, the same optimization model and algorithm parameters are used to solve the problem, so as to complete the system capacity configuration, operation scheduling and economic analysis. In order to ensure comparability, the total installed capacity of renewable energy of the three systems is limited to 50 MW, while the capacity of energy storage system, electrolyzer, hydrogen storage tank and fuel cell is allowed to be adaptively optimized. The related results are summarized in Table 4.

Table 4. Comparison of Multi-Energy System Operation Results

Indicator	Case 1 (Wind–Storage–Hydrogen)	Case 2 (PV–Storage–Hydrogen)	Case 3 (Wind–PV–Storage–Hydrogen)
Installed capacity (MW)	47.9 (Wind)	45.6 (PV)	Wind 26.8 / PV 21.5
Storage capacity (MWh)	94.3	102.7	88.5
Electrolyzer capacity (MW)	23.8	21.2	25.4
Hydrogen storage (t)	38.9	35.6	41.7
Fuel cell capacity (MW)	13.7	14.5	12.8
Total system cost ($\times 10^8$ CNY)	4.57	4.83	4.41
LCOE (CNY/kWh)	0.438	0.462	0.421
Annual hydrogen production (10^3 Nm^3)	68.9	62.3	72.6

From Table 4, different renewable energy configurations have significant impacts on system operational performance and economic indicators. In Case 1, due to the strong randomness and fluctuation of wind power, the system needs to be equipped with higher capacity energy storage and hydrogen storage devices to maintain the balance between supply and demand, resulting in the total cost of the system reaching 4.57×10^8 CNY. In contrast, the photovoltaic output of Case 2 shows obvious daily cycle characteristics, but there is no power output at night, which makes the system more dependent on energy storage and fuel cells. The energy storage capacity is increased to 102.7 MWh, and the LCOE is 0.462 CNY/kWh, which is relatively low in economy. Compared with a single energy system, Case 3 (Wind-Solar Complementary System) shows better comprehensive performance. The complementarity of wind power and photovoltaic in time scale effectively reduces the fluctuation of renewable energy output, thus reducing the dependence on energy storage system (the energy storage capacity is reduced to 88.5 MWh). Additionally, the coordinated operation of the system improves the utilization rate of electrolyzer, and the annual hydrogen production is increased to 72.6× 10 nm, which is 5.37% higher than that of Case 1. In terms of economy, the total cost of the system is reduced to 4.41× 10 CNY (3.5% lower than that of the wind power system), and the LCOE is reduced to 0.421 CNY/kWh (3.88% lower). Generally speaking, the wind-solar hybrid system is superior to the single energy system in reducing energy waste, improving hydrogen energy utilization efficiency and improving economic performance, which verifies the applicability and superiority of the IHBA-MIP framework in multi-energy coupling scenarios. Additionally, it also shows that the reasonable introduction of photovoltaic resources can further improve the operational stability and economic benefits of the electricity-hydrogen system.

3.5. Sensitivity and Robustness Analysis

In order to further evaluate the stability and adaptability of IHBA-MIP framework under the disturbance of key parameters and different meteorological conditions, sensitivity analysis and robustness analysis are carried out in this study. In the sensitivity analysis, two parameters that have significant influence on the system economy and operation performance are selected: the efficiency of electrolytic cell and the unit cost of hydrogen storage system. On the basis of its benchmark value, the disturbance range of 20% is imposed respectively, and the system is optimized again. The related results are summarized in Table 5.

Table 5. Sensitivity Analysis of Key System Parameters

Parameter	Value	Total system cost ($\times 10^8$ CNY)	LCOE (CNY/kWh)	Annual hydrogen production (10^3 Nm^3)	Payback period (years)
Electrolyzer efficiency	0.57	4.92	0.468	54.3	21.6
	0.64	4.73	0.452	61.7	19.8
	0.71	4.57	0.438	68.9	18.4
	0.78	4.39	0.423	74.6	17.1
	0.85	4.26	0.412	80.8	15.9
Hydrogen storage unit cost	52 CNY/kg	4.49	0.432	70.5	17.6
	65 CNY/kg	4.57	0.438	68.9	18.4
	78 CNY/kg	4.66	0.445	67.2	19.3

As shown in Table 5, when the efficiency of electrolyzer is increased from 0.57 to 0.85, the total cost of the system is reduced from 4.92×10^8 CNY to 4.26×10^8 CNY, with a decrease of 13.4%, and the LCOE is reduced by about 12%. This shows that the efficiency of electrolyzer is the core parameter affecting the system economy. In contrast, when the unit cost of hydrogen storage system changes from 52 CNY/kg to 78 CNY/kg, only about 3.8% of the total cost of the system fluctuates; In the range of 20% cost disturbance, the total cost change is about 2%, which shows that the system has strong robustness to the change of hydrogen storage cost.

In addition, this study further analyzes the influence of IHBA algorithm parameters on the optimization performance. The population size and the maximum number of iterations are selected as key sensitivity parameters. Under the condition that other parameters remain unchanged, the population size is set to [20, 30, 40] and the maximum number of iterations is set to [100, 150, 200, 250] respectively, and the corresponding optimal fitness value and convergence time are recorded. The related results are summarized in Table 6.

Table 6. Sensitivity Analysis of IHBA Algorithm Parameters

Population size	Maximum iterations	Optimal fitness	Convergence time (s)
20	100	0.486	42.3
20	150	0.463	58.7
20	200	0.451	73.5
20	250	0.447	89.6
30	100	0.459	64.2
30	150	0.438	78.9
30	200	0.424	91.5
30	250	0.420	109.8
40	100	0.452	85.6
40	150	0.431	103.4
40	200	0.419	128.4
40	250	0.417	156.7

The results in Table 6 show that with the increase of population size and iteration times, the optimal fitness of the algorithm gradually decreases, indicating that the optimization performance is improved. When the population size is increased from 20 to 30 and the number of iterations is set to 200, the fitness decreases from 0.451 to 0.424, and the optimization performance is improved by about 6.0%. When the population size is further increased to 40 and the number of iterations is increased to 250, the fitness is only reduced from 0.424 to 0.417, the improvement range is less than 2%, and the calculation time is increased by about 71.3%. Additionally, when the number of iterations exceeds 200, further improvements in optimization are minimal, indicating that the algorithm has essentially converged. Considering both accuracy and computational efficiency, a population size of 30 and 200 iterations were selected as the optimal parameter combination.

For robustness analysis, wind power and load data from the Mongolian Eastern region (2022, 2023, and 2024) were used for comparative simulations. Under identical model and algorithm parameter settings, the variations in system configuration and operational performance indicators were analyzed. The results are presented in Table 7.

Table 7. System Operation Results under Meteorological Data from Different Years

Indicator	2022	2023	2024
Installed Capacity (MW)	46.5	48.7	47.9
Energy Storage Capacity (MWh)	97.2	92.1	94.3
Electrolyzer Capacity (MW)	22.9	24.5	23.8
Total System Cost ($\times 10^8$ CNY)	4.63	4.52	4.57
LCOE (CNY/kWh)	0.444	0.433	0.438

As shown in Table 7, under different annual meteorological conditions, the optimal configuration of the system only shows small fluctuations. The installed capacity of wind power varies between 46.5-48.7 MW, with the maximum deviation of 4.73% and the fluctuation range of energy storage capacity of 5.25%. The maximum deviation of the total cost of the system is 2.38%, and the change range of LCOE is controlled within 0.011 CNY/kWh. Overall, the results show that the IHBA-MIP framework can still maintain a stable optimal solution and good economic performance under the disturbance of key parameters and different meteorological conditions. The system is relatively sensitive to electrolytic cell efficiency, but it is robust to hydrogen storage cost and meteorological fluctuation, which shows its adaptability and reliability in practical engineering applications.

3.6. Ablation Experiment

Ablation experiments are designed to compare different algorithm structures and verify the effectiveness of IHBA improvement strategies. Under the unified system model and constraints, four algorithm variants are constructed: original HBA, HBA-C initialized by Bernoulli chaotic map, HBA-N with nonlinear decreasing parameters, and completely improved IHBA. All algorithms adopt the same parameter settings and run independently for 30 times, and average the results to weaken the randomness. The experimental results are shown in Table 8.

Table 8. Ablation Experiment Results

Algorithm	Best Fitness Value	Average Fitness Value	Standard Deviation	Convergence Time (s)
HBA	0.461	0.472	0.018	88.6
HBA-C	0.438	0.447	0.013	90.2
HBA-N	0.432	0.441	0.011	92.5
IHBA	0.424	0.431	0.008	91.5

As shown in Table 8, all the improvement strategies have a positive impact on the performance of the algorithm. Compared with the original HBA, HBA-C with chaotic mapping initialization reduces the optimal fitness value from 0.461 to 0.438, increasing by 4.99%, indicating that the quality of population initialization has been improved, thus enhancing the global search ability of the algorithm. On this basis, after HBA-N further introduces nonlinear decreasing parameters, the optimal fitness value is reduced to 0.432, which is 6.29% higher than that of HBA, indicating that this strategy is helpful to balance global exploration and local development and improve convergence accuracy. The completely improved IHBA has the best performance, and its optimal fitness value reaches 0.424, which is 8.0% higher than the original HBA and 8.69% lower in average fitness. In terms of convergence time, there is little difference among the improved algorithms. Compared with HBA, IHBA only increases the calculation time by 3.27%, but obtains significantly better optimization results. This shows that the improved strategy can improve the performance of the algorithm, while the computational overhead is still within an acceptable range. Generally speaking, chaotic mapping mainly enhances population diversity, and nonlinear decreasing parameters improve local search ability. The synergy between them makes IHBA superior to other variants in convergence accuracy and stability, thus verifying the effectiveness and necessity of the proposed improved method.

3.7. Discussion

In this study, a double-layer capacity-operation optimization model of wind-storage-hydrogen-gas turbine system is constructed, in which the upper layer uses IHBA to search for the optimal capacity combination, and the lower layer uses MIP model to accurately describe the equipment operation constraints, thus realizing the collaborative solution of capacity planning and operation optimization. The results show that the ability of IHBA to explore the solution space in the capacity search stage is significantly enhanced by introducing Bernoulli chaos initialization, piecewise nonlinear decreasing parameters and transverse crossover strategy. Combined with operation optimization, the operation efficiency and economic performance of the system are further improved: LCOE is reduced, dynamic payback period is shortened, and hydrogen production is increased, which reflects the synergistic gain effect between capacity adjustment and scheduling strategy. The results show that the double-layer framework keeps its advantages in the coupling between capacity and operation, and significantly improves the coordination of energy flow among subsystems.

Compared with similar researches on electric-hydrogen coupling (P2H) systems at home and abroad, most of the existing researches mainly focus on single-layer capacity optimization or operation scheduling optimization, or adopt simplified operation model in capacity planning, so it is difficult to fully describe the feedback effect of operation constraints on capacity allocation. For example, some studies mainly use deterministic or robust optimization methods for capacity planning. Although uncertainty can be considered, the global search ability for complex nonlinear problems is limited. Other studies focus on operation scheduling optimization, and capacity allocation often depends on empirical setting or step-by-step solution, lacking a unified optimization framework. In contrast, this study realizes the deep integration of IHBA and MIP, and makes heuristic global search and precise mathematical programming achieve collaborative optimization. This method not only ensures the solution accuracy, but also improves the optimization efficiency, so that the capacity scheme can better adapt to the actual operation requirements.

Compared with the existing research, this study has a clear research focus and complementary significance. Deng et al. realized the collaborative optimization of capacity-operation at the level of microgrid cluster by building a shared electricity-hydrogen hybrid energy storage station, emphasizing the economic benefits brought by the sharing mechanism [18]. This study focuses on the single wind-storage-hydrogen-gas turbine system, and improves the capacity allocation accuracy and operation optimization efficiency through the double-layer coupling structure. Lv et al. investigated robust capacity planning for PV–battery–hydrogen systems under green certificate trading and demand fluctuations, emphasizing uncertainty and risk avoidance [19], whereas this study highlights the deep integration of heuristic search and operational optimization to enhance the economic feedback mechanism of capacity schemes. Li et al. developed a distributed robust optimization model for electricity–hydrogen hybrid storage in interacting multi-microgrid systems. Their model accounted for uncertainties in wind and solar generation. The study showed that reducing hydrogen storage investment costs is crucial for improving the system's economic performance [20]. This study further emphasizes the feedback effect of operational logic on capacity planning, indicating that considering only static investment cannot achieve system-level optimality; the bidirectional interaction between capacity and operation must be strengthened. Moreover, from the perspective of system architecture, most existing studies focus on the "wind–storage–hydrogen" or "solar–storage–hydrogen" configurations. In this study, a hydrogen-blended gas turbine is further introduced as a peaking and backup power source. This not only enhances the system's power supply reliability under extreme load conditions but also enables carbon reduction and cascade energy utilization through hydrogen use. This multi-coupling structure of "renewable energy-energy storage-hydrogen energy-thermal power unit" enables the system to achieve a better balance between flexibility and economy.

Generally speaking, although a lot of research has focused on the shared energy storage mechanism, demand uncertainty or sensitivity analysis of investment cost, this study has constructed an integrated capacity-operation optimization framework based on the "algorithm-operation" coupling architecture, which provides a new research idea for wind-storage-hydrogen-gas turbine system planning. Its main advantage lies in improving the consistency of capacity search accuracy and operation decision additionally. The future research can further explore the multi-agent collaborative modeling method and the characterization mechanism of operational uncertainty, and provide an expanding direction for subsequent related research.

4. Conclusions

Aiming at the configuration problem of wind-storage-hydrogen-gas turbine (Wind-storage-H-GT) collaborative system, this study puts forward a two-layer optimization framework integrating IHBA and MIP, and analyzes it based on the real wind power data of a certain area in eastern Inner Mongolia. The results show that IHBA has fast convergence speed and strong global search ability in capacity optimization, and its fitness value reaches the optimal value of 0.424 after 100 iterations, which is better than PSO, GA and HBA, reflecting its high efficiency and stability in global optimal solution search. In terms of optimal capacity configuration, the scheme obtained by IHBA includes 47.9 MW wind power installed capacity, 94.3 MWh battery energy storage, the largest hydrogen storage system and the smallest hydrogen-doped gas turbine capacity. The total cost of the system is 4.57×10^{8} CNY, which is the lowest among the four algorithms, indicating that it achieves a good balance between capacity allocation and economy. The operation results show that the electrolyzer, fuel cell and gas turbine can cooperate effectively, and the hydrogen storage device switches smoothly between hydrogen production and hydrogen consumption. At the end of the month, the SOH fluctuated between 0.2 and 0.8, and the battery and hydrogen energy storage effectively suppressed the fluctuation of wind power, making the annual wind rejection rate low, the system running stably and the wind power utilization rate high. The economic analysis shows that the LCOE is reduced to 0.438 CNY/kWh, the annual hydrogen production is increased to 68,900 standard cubic meters, and the dynamic payback period is shortened to 18.4 years after the introduction of the operation control strategy, which verifies the significant role of operation scheduling in cost optimization and investment recovery. The comparative analysis of multiple energy sources further shows that the wind-solar hybrid system can further reduce power abandonment and improve economic performance. Sensitivity and robustness analysis show that the system can still maintain stable optimal structure and good operation performance under the disturbance of key parameters and different annual meteorological conditions. Ablation experiments verify the effectiveness of IHBA's improved strategies in improving convergence speed, optimization accuracy and algorithm stability, which provides more reliable theoretical support for system design.

However, there are still some limitations in this study. The scheduling flexibility brought by power flow coupling between multiple regions and cross-regional energy exchange is not considered, which makes the system closer to the isolated island operation scene; The space-time complementarity of photovoltaic, hydropower and other renewable energy sources is not included, which limits the exploitation of multi-energy synergy potential; Long-term meteorological uncertainty, hydrogen load fluctuation and equipment degradation are not systematically modeled, which limits the robustness of the model search space; In addition, the solution time of MIP may increase exponentially under large-scale problems, which affects the scalability of the model; The setting of IHBA parameters is still sensitive, which may lead to the fluctuation of convergence speed and global search performance under different system structures. The future research can be further extended to multi-energy and multi-regional collaborative optimization framework, introducing multi-energy complementary mechanisms such as wind, light, water and fire, and coupling electricity-hydrogen dual network with demand response, so as to improve the overall flexibility and uncertainty adaptability of the system. Additionally, this study can explore the adaptive parameter adjustment mechanism of IHBA, and combine parallel computing, distributed solution and agent model acceleration methods to significantly reduce the calculation cost and improve the real-time performance and engineering feasibility of capacity allocation and operation scheduling.

References

[1] Tonelli D, Rosa L, Gabrielli P, et al. Global land and water limits to electrolytic hydrogen production using wind and solar resources. Nat Commun. 2023;14(1):5532.

[2] Vargas-Ferrer P, Álvarez-Miranda E, Tenreiro C, et al. Integration of high levels of electrolytic hydrogen production: Impact on power systems planning. J Clean Prod. 2023;409:137110.

[3] Han X, Shi M, Wang G, et al. Optimal Control of Wind-Photovoltaic-Hydropower-Hydrogen Complementary System Considering Operation State of Hydropower Units. SSRN 5200642.

[4] Hu G, Zhao X, Cheng S, et al. The Optimal Configuration of Energy Storage Capacity Based on the NSGA-II Algorithm and Electrochemical Energy Storage Operational Modes. Processes. 2025;13(5):1432.

[5] Dong Y, Han Z, Li C, et al. Research on the optimal planning method of hydrogen-storage units in wind–hydrogen energy system considering hydrogen energy source. Energy Rep. 2023;9:1258-1264.

[6] Asim AM, Awad ASA, Attia MA. Integrated optimization of energy storage and green hydrogen systems for resilient and sustainable future power grids. Sci Rep. 2025;15(1):25656.

[7] Bryan J, Meek A, Dana S, et al. Modeling and design optimization of carbon-free hybrid energy systems with thermal and hydrogen storage. Int J Hydrogen Energy. 2023;48(99):39097-39111.

[8] Avilés FN, Etchepare RM, Aguayo MM, et al. A mixed-integer programming model for an integrated production planning problem with preventive maintenance in the pulp and study industry. Eng Optim. 2023;55(8):1352-1369.

[9] Thomas M, Sela L. A Mixed-Integer Linear Programming Framework for Optimization of Water Network Operations Problems. Water Resour Res. 2024;60(2):e2023WR034526.

[10] Xing L, Liu Y. An optimization capacity design method of wind/photovoltaic/hydrogen storage power system based on PSO-NSGA-II. Energy Eng. 2023;120(4):1023-1043.

[11] Liu Z, Ma R, Yu X, et al. A capacity planning method for energy storage equipment of an integrated energy system including hydrogen storage, based on an oxygen sales mechanism. Int J Hydrogen Energy. 2025;177:151535.

[12] Modu B, Abdullah MP, Bukar AL, et al. Energy management and capacity planning of photovoltaic-wind-biomass energy system considering hydrogen-battery storage. J Energy Storage. 2023;73:109294.

[13] Xia Q, Zou Y, Wang Q. Optimal Capacity Planning of Green Electricity-Based Industrial Electricity-Hydrogen Multi-Energy System Considering Variable Unit Cost Sequence. Sustainability. 2024;16(9):3684.

[14] Yang B, Zheng R, Wang J, et al. Optimal control of hybrid wind-storage-hydrogen system based on wind power output prediction. J Energy Storage. 2024;104:114432.

[15] Yang J, Chi H, Cheng M, et al. Performance analysis of hydrogen supply using curtailed power from a solar-wind-storage power system. Renew Energy. 2023;212:1005-1019.

[16] Hu G, Zhong J, Wei G. SaCHBA_PDN: Modified honey badger algorithm with multi-strategy for UAV path planning. Expert Syst Appl. 2023;223:119941.

[17] Liu X, Xu Y, Wang T, et al. An adaptive search strategy combination algorithm based on reinforcement learning and neighborhood search. J Comput Des Eng. 2025;12(2):177-217.

[18] Deng H, Wang J, Shao Y, et al. Optimization of configurations and scheduling of shared hybrid electric-hydrogen energy storages supporting to multi-microgrid system. J Energy Storage. 2023;74:109420.

[19] Lv X, Li X, Xu C. A robust optimization model for capacity configuration of PV/battery/hydrogen system considering multiple uncertainties. Int J Hydrogen Energy. 2023;48(21):7533-7548.

[20] Li J, Xiao Y, Lu S. Optimal configuration of multi microgrid electric hydrogen hybrid energy storage capacity based on distributed robustness. J Energy Storage. 2024;76:109762.